Electronic Supplementary Material (ESI) for Materials Chemistry Frontiers.

Dispiroacridine-indacenobisthiophenes positional isomers: Impact of the bridge on the physicochemical properties

Jean-David Peltier,[a] Benoît Heinrich,[b] Bertrand Donnio,[b] Olzhas A. Ibraikulov,[c] Thomas Heiser,[c] Nicolas Leclerc,[d] Joëlle Rault-Berthelot,*[a] and Cyril Poriel*[a]

[a] Univ Rennes, CNRS, ISCR-UMR CNRS 6226, F-35000 Rennes, France

[b] Institut de Physique et Chimie des Matériaux de Strasbourg, UMR 7504, CNRS-Université de Strasbourg, F- 67034 Strasbourg, France

[c] Laboratoire ICube, UMR 7357, CNRS-Université de Strasbourg, F-67087 Strasbourg, France

[d] Institut de Chimie et Procédés pour l'Energie, l'Environnement et la Santé (ICPEES), UMR 7515, CNRS-Université de Strasbourg, F-67087 Strasbourg, France

1 General experimental methods

1.1 Synthesis

All manipulations of oxygen and moisture-sensitive materials were conducted with a standard Schlenk technique. Commercially available reagents and solvents were used without further purification other than those detailed below. THF was obtained through a PURE SOLV™ solvent purification system. Analytical thin layer chromatography was carried out using aluminum backed plates coated with Merck Kieselgel 60 GF254 and visualized under UV light (at 254 and 360 nm). Flash chromatography was carried out using Teledyne Isco CombiFlash® Rf 400 (UV detection 200-360nm), over standard silica cartridges (Redisep® Isco or Puriflash® columns Interchim). ^{1}H and ^{13}C NMR spectra were recorded using Bruker 300 MHz instruments (^{1}H frequency, corresponding ^{13}C frequency: 75 MHz); chemical shifts were recorded in ppm and J values in Hz. The residual signals for the NMR solvents used are 5.32 ppm (proton) and 54.00 ppm (carbon) for CD2Cl2 and 7.26 ppm (proton) for $CDCl_3$. High resolution mass spectra were recorded at the Centre Régional de Mesures Physiques de l'Ouest (CRMPO-Rennes) on a Bruker MaXis 4G.

1.2 Spectroscopic studies

Cyclohexane (spectroscopic grade, Acros), THF (spectroscopic grade, Merck), chloroform (spectroscopic grade, Merck), 1N solution of sulfuric acid in water (Standard solution, Alfa Aesar), and quinine sulfate dihydrate (99+%, ACROS organics) were used without further purification. UV-visible spectra were recorded using an UV-Visible spectrophotometer SHIMADZU UV-1605. Molar extinction coefficients (ε) were calculated from the gradients extracted from the plots of absorbance *vs* concentration with five solutions of different concentrations for each sample. Thin films were prepared by spin-coating ca 300 µL of a THF solution (1 mg/mL) on a sapphire plate (10 mm x 10 mm) at 2500 tr/min on a Süss$_+$MicroTec Lab Spin 6/8. IR spectra were recorded on a Bruker Vertex 7 0 using a diamond crystal MIRacle ATR (Pike).

1.3 Electrochemical studies

Electrochemical experiments were performed under argon atmosphere using a Pt disk electrode (diameter 1 mm). The counter electrode was a vitreous carbon rod. The reference electrode was either a silver wire in a 0.1 M $AgNO_3$ solution in CH_3CN for the studies in oxidation or a Silver wire coated by a thin film of AgI (silver(I)iodide) in a 0.1 M Bu_4NI solution in DMF for the studies in reduction. Ferrocene was added to the electrolyte solutions at the end of a series of experiments. The ferrocene/ferrocenium (Fc/Fc^+) couple served as internal standard. The three electrodes cell was connected to a PAR Model 273 potentiostat/galvanostat (PAR, EG&G, USA) monitored with the ECHEM Software. Activated Al_2O_3 was added in the electrolytic solution to remove excess moisture. For a further comparison of the electrochemical and optical properties, all potentials are referred to the SCE electrode that was calibrated at –0.405 V *vs.* Fc/Fc^+ system. Following the work of Jenekhe,[1] we estimated the electron affinity (EA) or lowest unoccupied molecular orbital (LUMO) and the ionization potential (IP) or highest occupied molecular orbital (HOMO) from the redox data. The LUMO level was calculated from: LUMO (eV) = $-[E_{onset}^{red}$ (*vs* SCE) + 4.4] and the HOMO level from: HOMO (eV) = $-[E_{onset}^{ox}$ (*vs* SCE) + 4.4], based on an SCE energy level of 4.4 eV relative to the vacuum. The electrochemical gap was calculated from: ΔE^{el} =|HOMO-LUMO| (in eV).

1.4 Molecular modelling

Full geometry optimization of the ground state and frequency calculation were performed with Density Functional Theory (DFT)[2,3] using the hybrid Becke-3 0 parameter exchange[4-6] functional and the Lee-Yang-Parr non-local correlation functional[7] (RB3LYP) implemented in the Gaussian 09 (Revision B.01) program suite[8] using the 6-31G+(d) basis set. Transition diagrams were obtained through TD-DFT calculations performed using the B3LYP functional and the 6-31G+(d) basis set on the geometry of S0. Figures were generated with GaussView 5.0.

1.5 Thermal analysis

Thermal Gravimetric Analysis (TGA) was carried out by using a Q50 apparatus of TA instruments at the Ecole Nationale Superieure de Chimie de Rennes. TGA curved were measured at 10°C/min from 0°C to 800°C under a nitrogen flux. Differential scanning calometry (DSC) was carried out by using a NETZSCH DSC 200 F3 instrument equipped with an intracooler. DSC traces were measured at 10°C/min under a nitrogen flux.

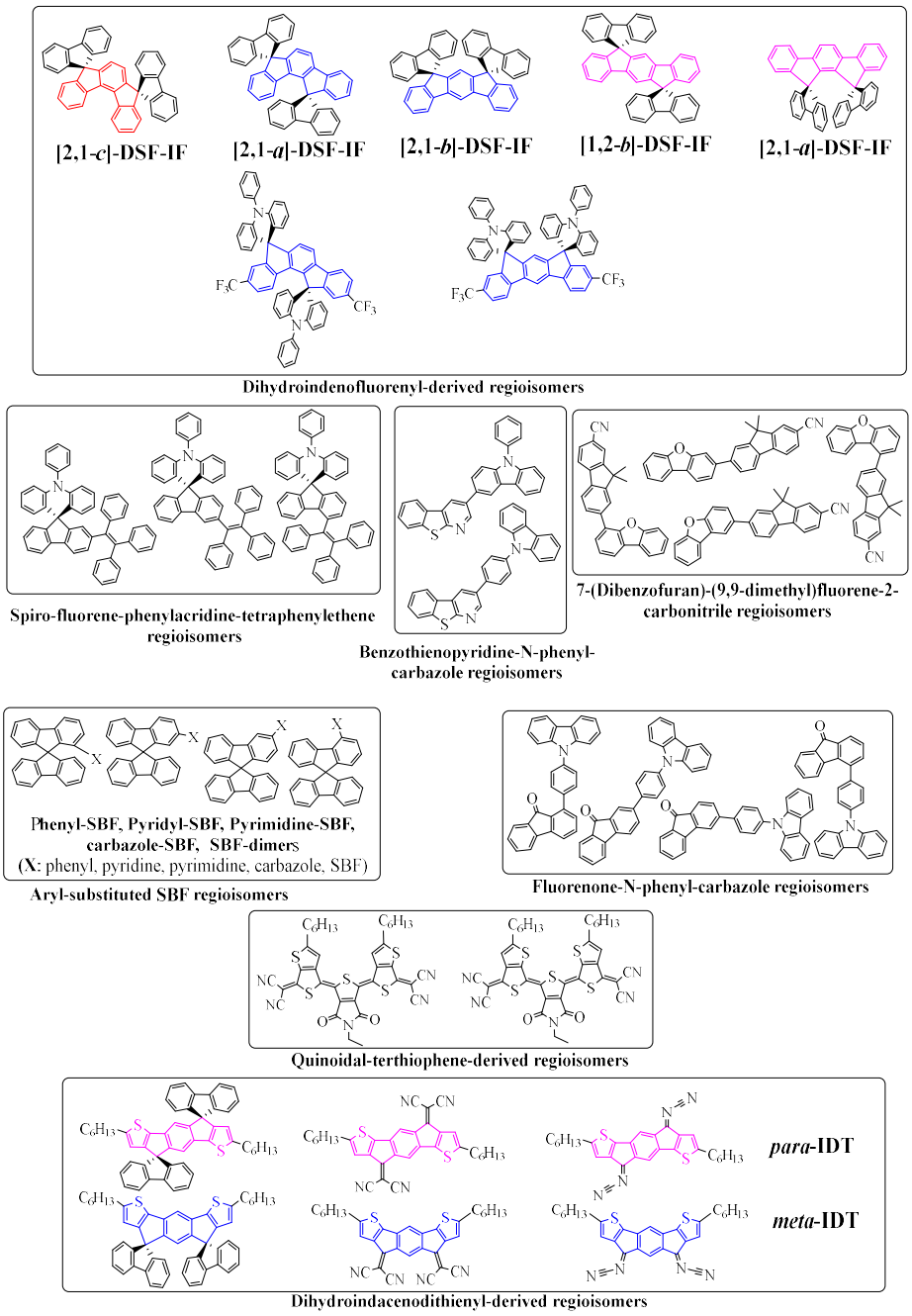

Chart S1. Positional isomerism in OSCs

2 Synthetic procedures

SPA-F was already described by us in 2020.[9]

The two diketones, ***para*-IDT(=O)$_2$** and ***meta*-IDT(=O)$_2$**, used as starting material for ***para*-DSPA-IDT** and ***meta*-DSPA-IDT** and for ***para*-IDT** and ***meta*-IDT** were previously described by us in 2017.[10]

2.1 General procedure for the synthesis of the two DSPA-IDT isomers

2-bromo-triphenylamine (0.975 mmol) was dissolved in dry THF (15 mL) and cooled down to -80°C. A 2.5 M hexane solution of n-BuLi (0.39 mL, 0.975 mmol) was then added dropwise into the solution at -80°C. The resulting mixture was stirred at the same temperature for 1 hour. Ketone (0.325 mmol), dissolved in dry THF (25 mL) was then added dropwise and the mixture

was allow to warm up till 20°C overnight. Brine (50ml) was added and the mixture extracted with ethyl acetate (3 X 50 ml). The combined organic extracts were dried over anhydrous magnesium sulfate, filtered and concentrated under reduced pressure.
The obtained residue was dissolved in dichloromethane (40ml) and then BF_3-etherate (500µl) was added. The resulting mixture was stirred at room temperature for 1h30. The solvent was then evaporated and the compound purified by flash chromatography on silica gel, eluting with a mixture of dichloromethane in petroleum ether. The compound was later recrystallized from a mixture of $CHCl_3$ with methanol.

2.1.1 Para-DSPA-IDT: 2',7'-dihexyl-10,10''-diphenyl-10H,10''H-dispiro[acridine-9,4'-s-indaceno[1,2-b:5,6-b']dithiophene-9',9''-acridine]

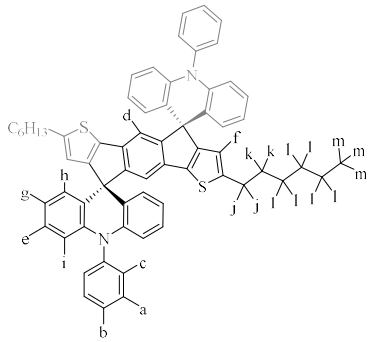

para-DSPA-IDT

The general procedure was performed with ***para*-IDT(=O)$_2$**[10] as the ketone. Recrystallization was performed in a mixture of chloroform in methanol to give a pale orange solid in a yield of 79% (236 mg, 0.26 mmol)

M.p. > 210 °C

^{1}H NMR (300 MHz, CD_2Cl_2) δ 7.77 (t, *J* = 7.6 Hz, 4H, Ha), 7.62 (td, *J* = 7.5 Hz, 2H, Hb), 7.57 – 7.50 (m, 4H, Hc), 7.39 (s, 2H, Hd), 6.97 (ddd, *J* = 8.6, 6.8, 2.0 Hz, 4H, He), 6.68 (d, *J* = 1.0 Hz, 2H, Hf), 6.63 (td, *J* = 7.3, 6.8, 1.1 Hz, 4H, Hg), 6.58 (dd, *J* = 7.7, 2.0 Hz, 4H, Hh), 6.40 (dd, *J* = 8.3, 1.1 Hz, 4H, Hi), 2.84 (t, *J* = 7.6 Hz, 4H, Hj), 1.67 (q, *J* = 7.4 Hz, 4H, Hk), 1.45 – 1.24 (m, 12H, Hl), 0.99 – 0.74 (m, 6H, Hm).

^{13}C NMR (75 MHz, CD_2Cl_2) δ 159.57 (C), 158.07 (C), 150.53 (C), 141.67 (C), 140.96 (C), 139.16 (C), 133.54 (C), 131.08 (CH) 131.06 (CH), 128.50 (CH), 127.33 (CH), 126.65 (CH), 123.69 (C), 120.59 (CH), 119.26 (CH), 115.10 (CH), 114.81 (CH), 54.69 (spiroC), 31.54 (CH_2), 31.47 (CH_2), 31.11 (CH_2), 28.67 (CH_2), 22.52 (CH_2), 13.75 (CH_3).

HRMS calculated for $C_{64}H_{56}N_2S_2$: 916.3885, found: 916.3879 [$M^{+\cdot}$]

IR (ATR, cm^{-1}):ν= 418, 447, 471, 503, 620, 661, 698, 721, 741, 827, 862, 939, 1056, 1161, 1269, 1328, 1446, 1475, 1589, 2850, 2923, 3029, 3066

λ_{abs} [nm] (ε[10^4 x $L.mol^{-1}.cm^{-1}$]) =264 (2.11), 277 (1.69), 296 (1.40), 342 (1.31), 359 (2.30), 377 (2.35)

Φ_{sol} (λ_{exc} [nm]) = 34 (359) (measured in cyclohexane)

2.1.2 Meta-DSPA-IDT: 2',8'-dihexyl-10,10''-diphenyl-10H,10''H-dispiro[acridine-9,4'-s-indaceno[1,2-b:7,6-b']-dithiophene-6',9''-acridine]

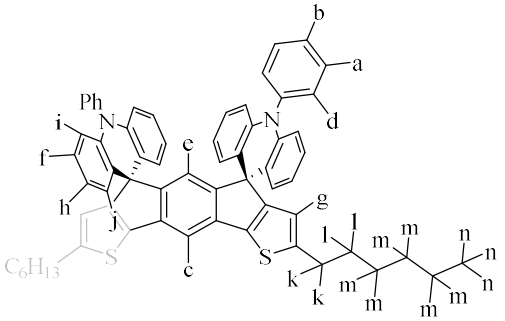

***Meta*-DSPA-IDT**

The general procedure was performed with ***meta*-IDT(=O)$_2$**[10] as the ketone. Recrystallization was performed in a mixture of chloroform in methanol to give a light yellow solid in a yield of 91% (270 mg, 0.29 mmol)

M.p. 178 °C

^{1}H NMR (300 MHz, CD_2Cl_2) 7.73 – 7.62 (m, 4H, Ha), 7.62 – 7.53 (m, 3H, Hb, Hc), 7.42 – 7.34 (m, 4H, Hd), 7.32 (d, *J* = 0.7 Hz, 1H, He), 6.91 (ddd, *J* = 8.6, 6.4, 2.4 Hz, 4H, Hf), 6.71 – 6.67 (m, 2H, Hg), 6.66 – 6.54 (m, 8H, Hh, Hi), 6.34 – 6.25 (m, 4H, Hj), 2.95 – 2.75 (m, 4H, Hk), 1.70 (q, *J* = 7.5 Hz, 4H, Hl), 1.47 – 1.23 (m, 12H, Hm), 1.01 – 0.85 (m, 6H, Hn)

^{13}C NMR (75 MHz, CD_2Cl_2) δ 161.33 (C), 157.07 (C), 150.91 (C), 141.51 (C), 140.91 (C), 137.96 (C), 135.97 (C), 131.09 (CH), 130.91 (CH), 128.32 (CH), 127.15 (CH), 126.93 (CH), 123.36 (CH), 120.33 (CH), 118.82 (CH), 114.5 (CH), 108.61 (CH), 54.81 (spiroC), 31.56 (CH_2), 31.48 (CH_2), 31.15 (CH_2), 28.86 (CH_2), 22.51 (CH_2), 13.76 (CH_3)

HRMS calculated for $C_{64}H_{56}N_2S_2$: 916.3885, found: 916.3878 [$M^{+\cdot}$]

IR (ATR, cm^{-1}): ν = 418, 447, 468, 621, 698, 742, 825, 856, 937, 1056, 1161, 1265, 1319, 1446, 1475, 1589, 2850, 2924, 3035, 3068

λ_{abs} [nm] (ε[10^4 x $L.mol^{-1}.cm^{-1}$]) = 283 (4.78), 293 (5.83), 304 (6.06), 332 (2.16), 340 (1.97), 349 (2.36), 367 (2.27)

Φ_{sol} (λ_{exc} [nm]) = 55 (349) (measured in cyclohexane)

2.2 General procedure for the synthesis of the two dihydroindacenodithiophene isomers ***Para*-dihexyl-IDT** and ***meta*-dihexyl-IDT** were prepared via a Wolff-Kishner reduction of their related diketones by hydrazine using a procedure reported by Wang and co-workers for DHIF synthesis.[11]

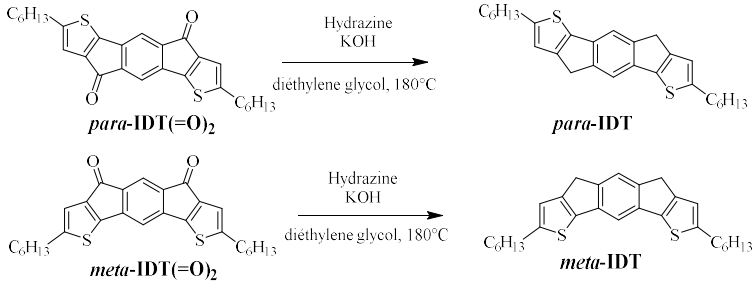

Potassium hydroxyde (20 eq) was added to a stirred solution of diketone (1 eq) suspended in diethylene glycol at room temperature. The Schlenk tube was degassed and hydrazine monohydrate (20 eq) was added via syringe. The reaction mixture was vigorously stirred at 180 °C under an argon atmosphere for 24 h. The hot solution was then poured into ice containing hydrochloric acid. The precipitate was filtered, washed with hexane and dried to give the IDT compound.

2.2.1 ***Para*-IDT**: 2,7-dihexyl-4,9-dihydro-s-indaceno[1,2-b:5,6-b']dithiophene
Potassium hydroxyde (121 mg, 2.15 mmol) was added to a stirred solution of ***para*-IDT(=O)2** (50 mg, 0.10 mmol) suspended in diethylene glycol (13 mL) at room temperature. The Schlenk tube was degassed and hydrazine monohydrate (98%, 0.11 ml, 2.16 mmol) was added via syringe. The reaction mixture was vigorously stirred at 180 °C under an argon atmosphere for 24 h. The hot solution was then poured into ice containing hydrochloric acid. The precipitate was filtered, washed with hexane and dried to give 8 mg of the title compound ***para*-IDT** (17%) as a yellow pale solid.

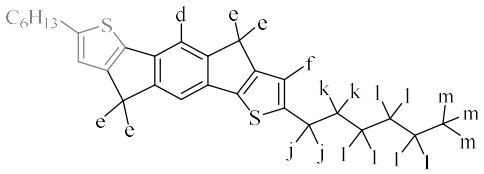

***para*-IDT**

^{1}H NMR (300 MHz; (CD_2Cl_2): ^{1}H NMR (300 MHz, CD_2Cl_2) δ 7.49 (s, 2H, H_d), 6.83 (s, 2H, H_f), 3.66 (s, 4H, H_e), 2.88 (s, 4H, H_j), 1.72 (p, J = 7.4 Hz, 4H, H_k), 1.43 – 1.20 (m, 12H, H_l), 0.96 – 0.84 (m, 6H, H_m).

2.2.2 ***Meta*-IDT**: 2,8-dihexyl-4,6-dihydro-s-indaceno[1,2-b:7,6-b']dithiophene
Potassium hydroxyde (728 mg, 13 mmol) was added to a stirred solution of ***meta*-IDT(=O)2** (3000 mg, 0.65 mmol) suspended in diethylene glycol (20 mL) at room temperature. The Schlenk tube was degassed and hydrazine monohydrate (98%, 0.64 mL, 13 mmol) was added via syringe. The reaction mixture was vigorously stirred at 180 °C under an argon atmosphere for 24 h. The hot solution was then poured into ice containing hydrochloric acid. The precipitate was filtered, washed with hexane and dried to give 8 mg of the title compound **meta-IDT** (3%) as a brown solid.

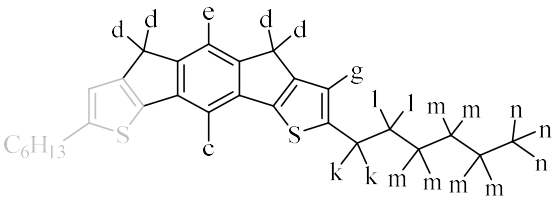

***Meta*-DSPA-IDT**

^{1}H NMR (300 MHz, $CDCl_3$) δ 7.47 (d, J = 24.5 Hz, 2H, H_c and H_e), 6.80 (s, 2H, H_g), 3.64 (s, 4H, H_d), 2.87 (t, J = 7.6 Hz, 4H, H_k), 1.80 – 1.65 (m, 4H, H_l), 1.43 – 1.19 (m, 12H, H_m), 0.94 – 0.83 (m, 6H, H_n).

3 Thermal properties

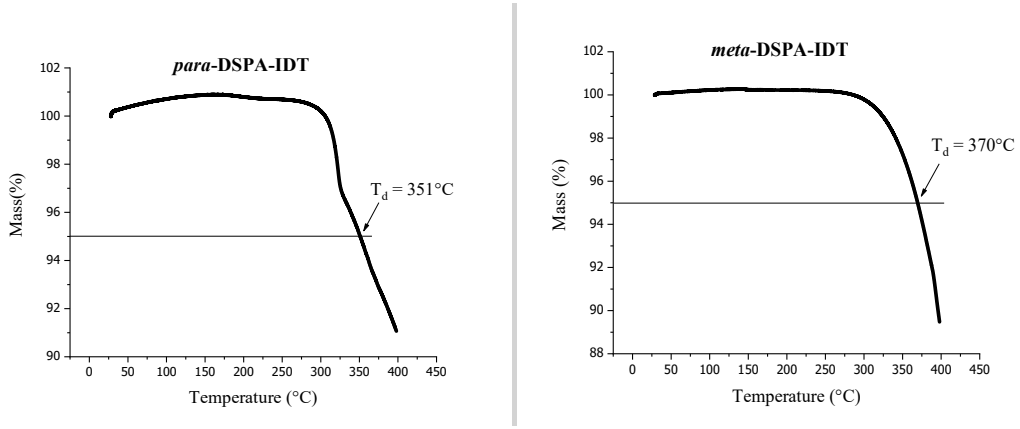

Figure S1. TGA analysis of ***para*-DSPA-IDT** and ***meta*-DSPA-IDT** under N_2 at 10°C.min^{-1}

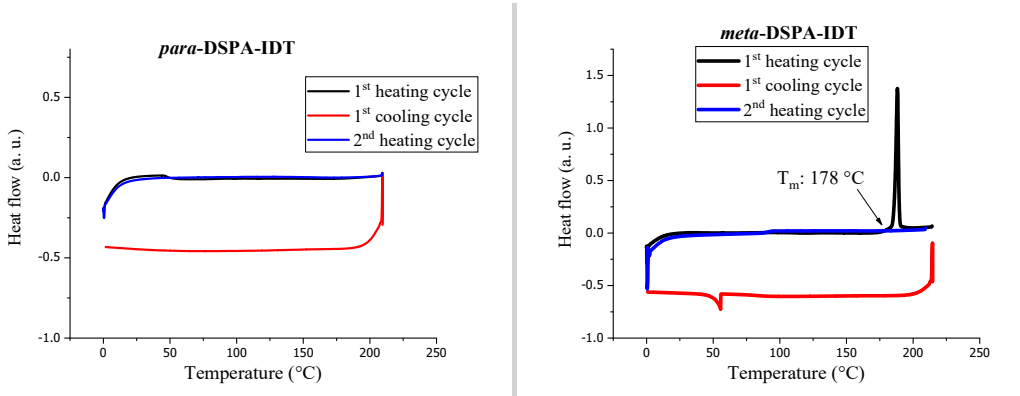

Figure S2. DSC analysis of ***para*-DSPA-IDT** and ***meta*-DSPA-IDT** under N_2 at 10°C.min^{-1}

4 Photophysical properties

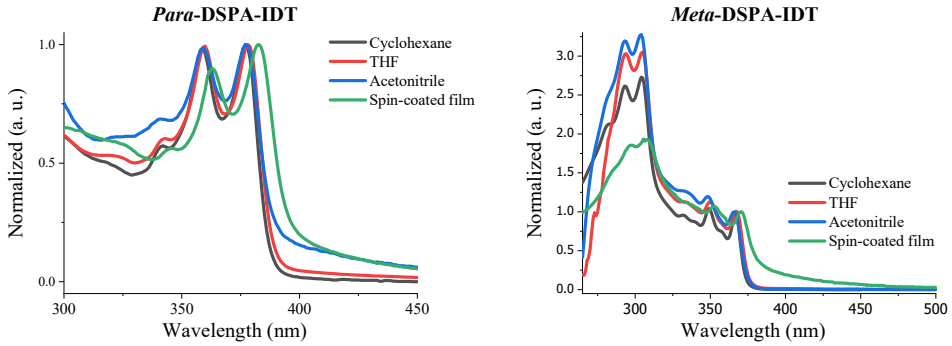

Figure S3. UV-vis absorption spectra of ***para*-DSPA-IDT** and ***meta*-DSPA-IDT** recorded in different solvents or as spin-coated film.

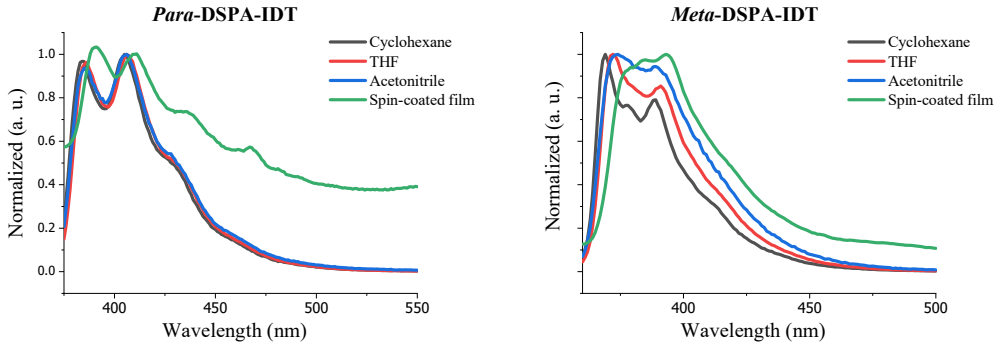

Figure S4. Emission spectra of ***para*-DSPA-IDT** and ***meta*-DSPA-IDT** recorded in different solvents or as spin-coated film.

5 Electrochemical studies

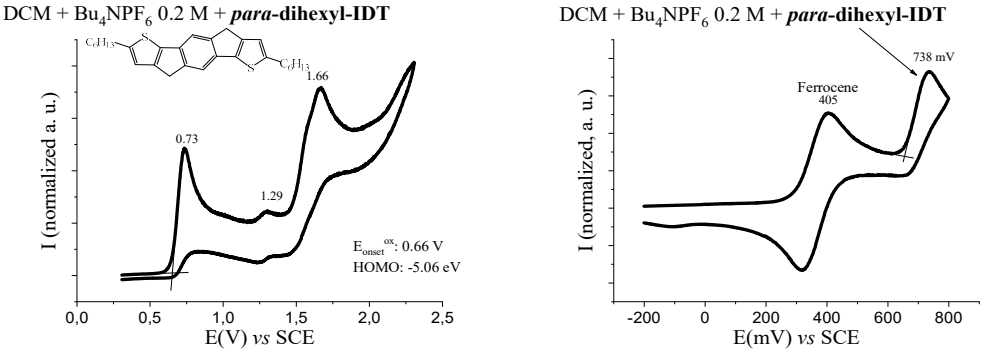

Figure S5. Cyclic voltammograms of (left) ***para*-dihexyl-IDT** recorded in the anodic range in DCM + Bu_4NPF_6 0.2 M and (right) in presence of ferrocene. Sweep-rate of 100 $mV.s^{-1}$, platinum disk (diameter 1mm) working electrode

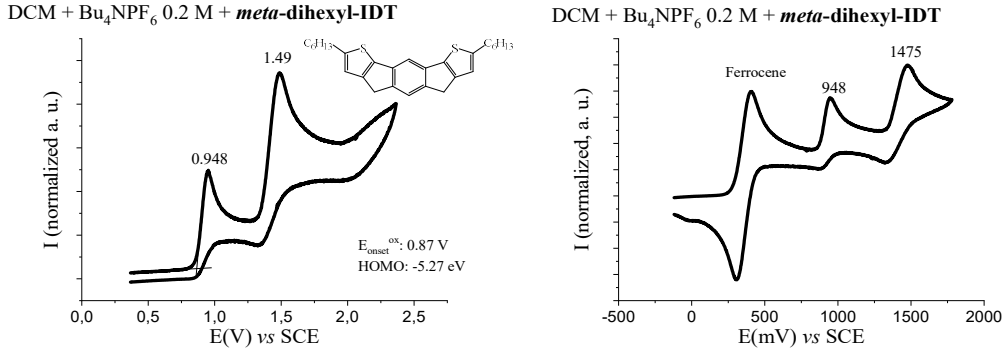

Figure S6. Cyclic voltammograms of (left) ***meta*-dihexyl-IDT** recorded in the anodic range in DCM + Bu_4NPF_6 0.2 M and (right) in presence of ferrocene. Sweep-rate of 100 $mV.s^{-1}$, platinum disk (diameter 1mm) working electrode

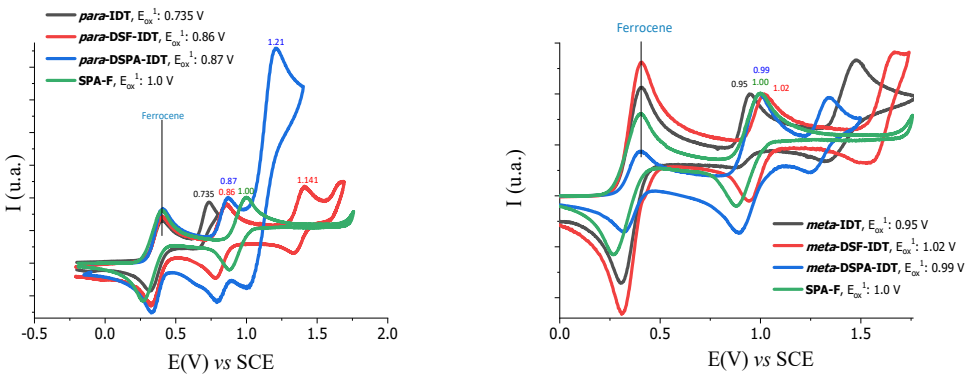

Figure S7. CVs recorded in Bu_4NPF_6 0.2 M in DCM in presence of ferrocene and normalized at the first oxidation wave of

- Left: ***para*-IDT** (black), ***para*-DSF-IDT** (red), ***para*-DSPA-IDT** (blue) and **SPA-F** (green)
- Right: ***meta*-IDT** (black), ***para*-DSF-IDT** (red), ***para* -DSPA-IDT** (blue) and **SPA-F** (green),

Sweep-rate 100 $mV.s^{-1}$. Working platinum disk electrode (Ø 1 mm).

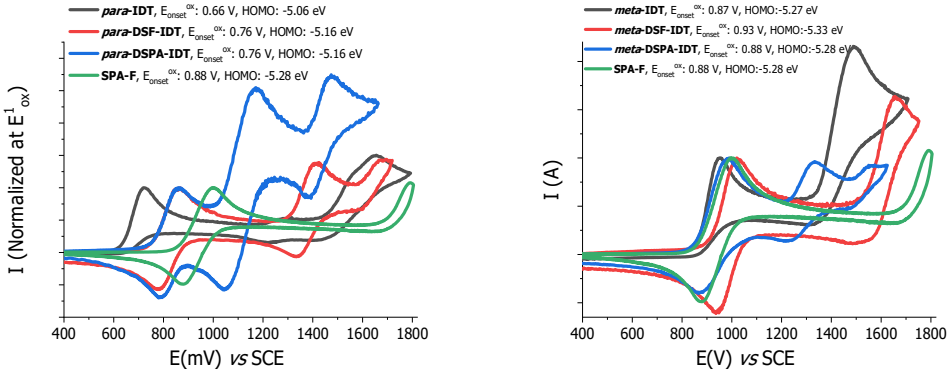

Figure S8. CVs recorded in Bu_4NPF_6 0.2 M in DCM and normalized at the first oxidation wave pointed in presence of ferrocene (see CVs above)

- Left: ***para*-IDT** (black), ***para*-DSF-IDT** (red), ***para*-DSPA-IDT** (blue) and **SPA-F** (green)
- Right: ***meta*-IDT** (black), ***para*-DSF-IDT** (red), ***para* -DSPA-IDT** (blue) and **SPA-F** (green),

Sweep-rate 100 $mV.s^{-1}$. Working platinum disk electrode (Ø 1 mm).

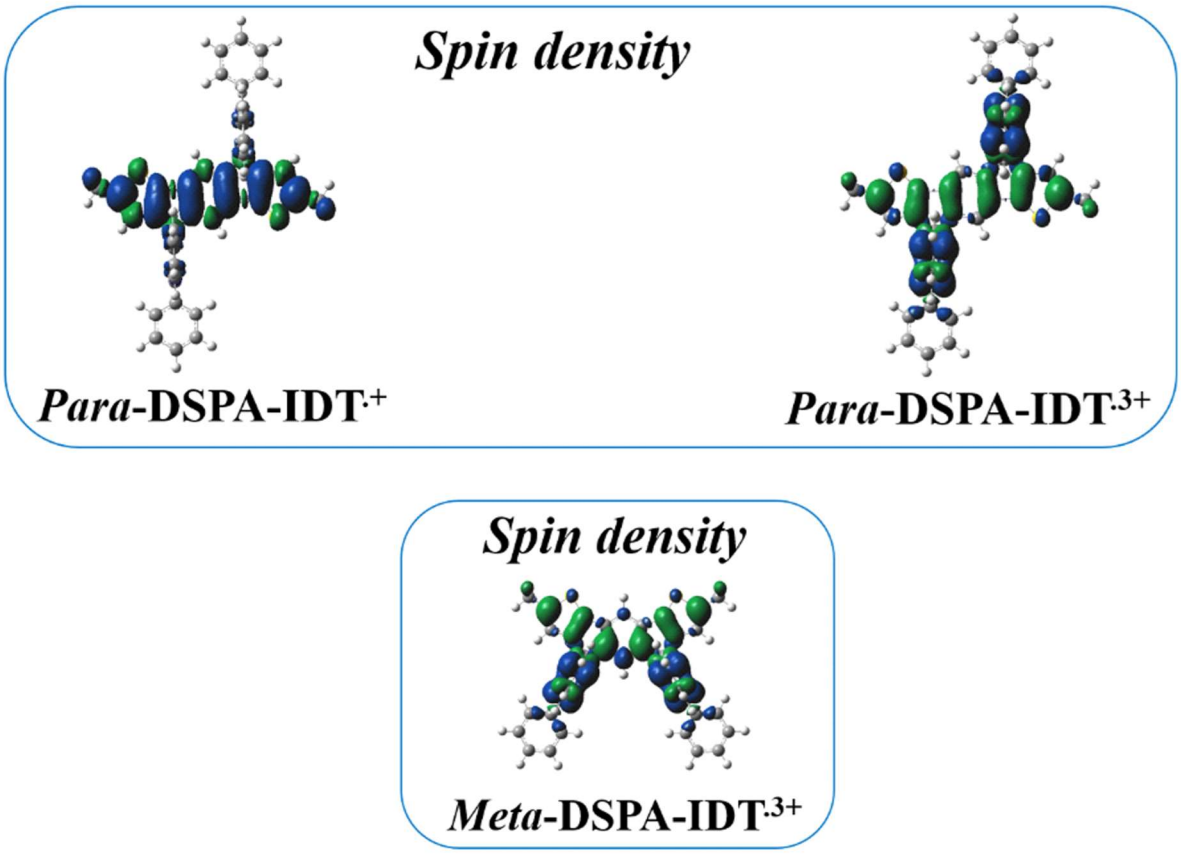

Figure S9. Plots of the Spin Density Distribution (SDD) of the radical cation and radical-trication of ***para*-DSPA-IDT(Me)$_2$** and of the radical-trication of ***meta*-DSPA-IDT(Me)$_2$** after geometry optimization with DFT B3LYP/6-31G + (d). SDD are shown with a cut-off of 0.001 e.bohr^{-3}.

6 COPY of NMR spectra

6.1 ^{1}H ***para*-IDT** in CD_2Cl_2

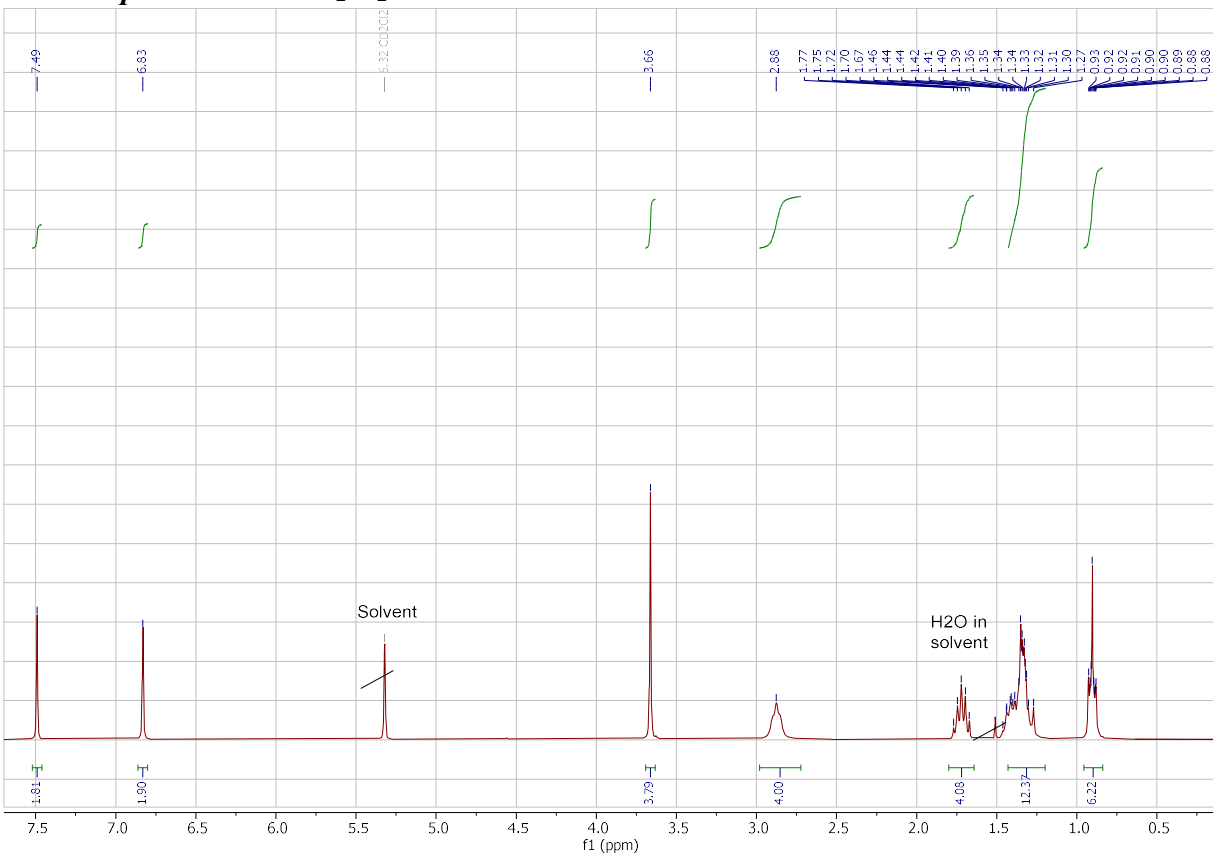

6.2 ^{1}H ***meta*-dihexyl-IDT** in $CDCl_3$

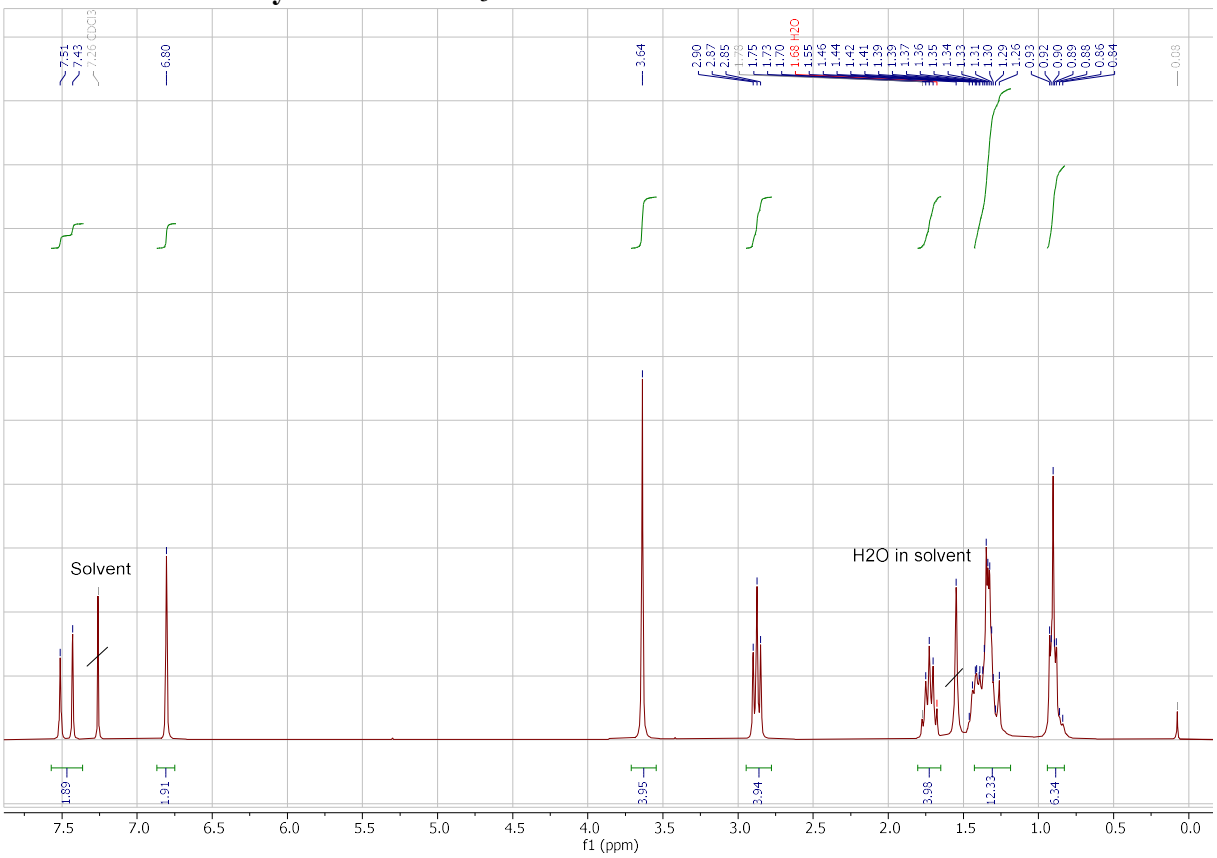

6.3 ***Para*-DSPA-IDT**

6.3.1 ^{1}H ***para*-DSPA-IDT** in CD_2Cl_2

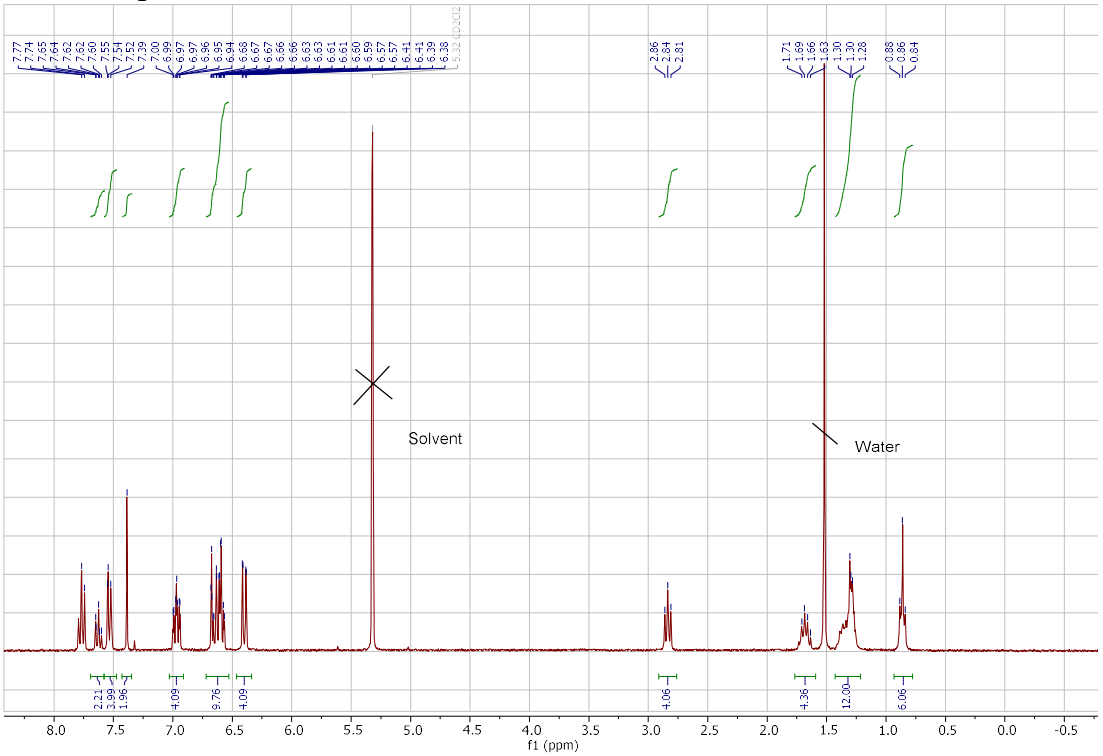

6.3.2 ^{13}C ***para*-DSPA-IDT**

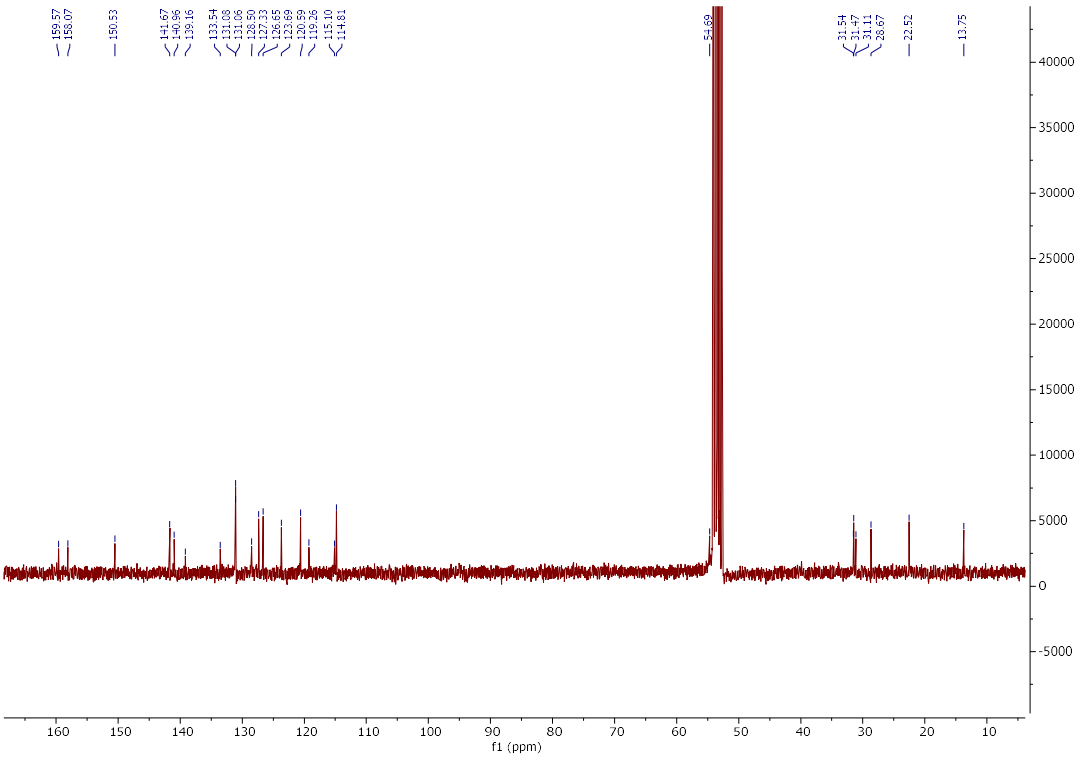

6.3.3 HSQC ***para*-DSPA-IDT**

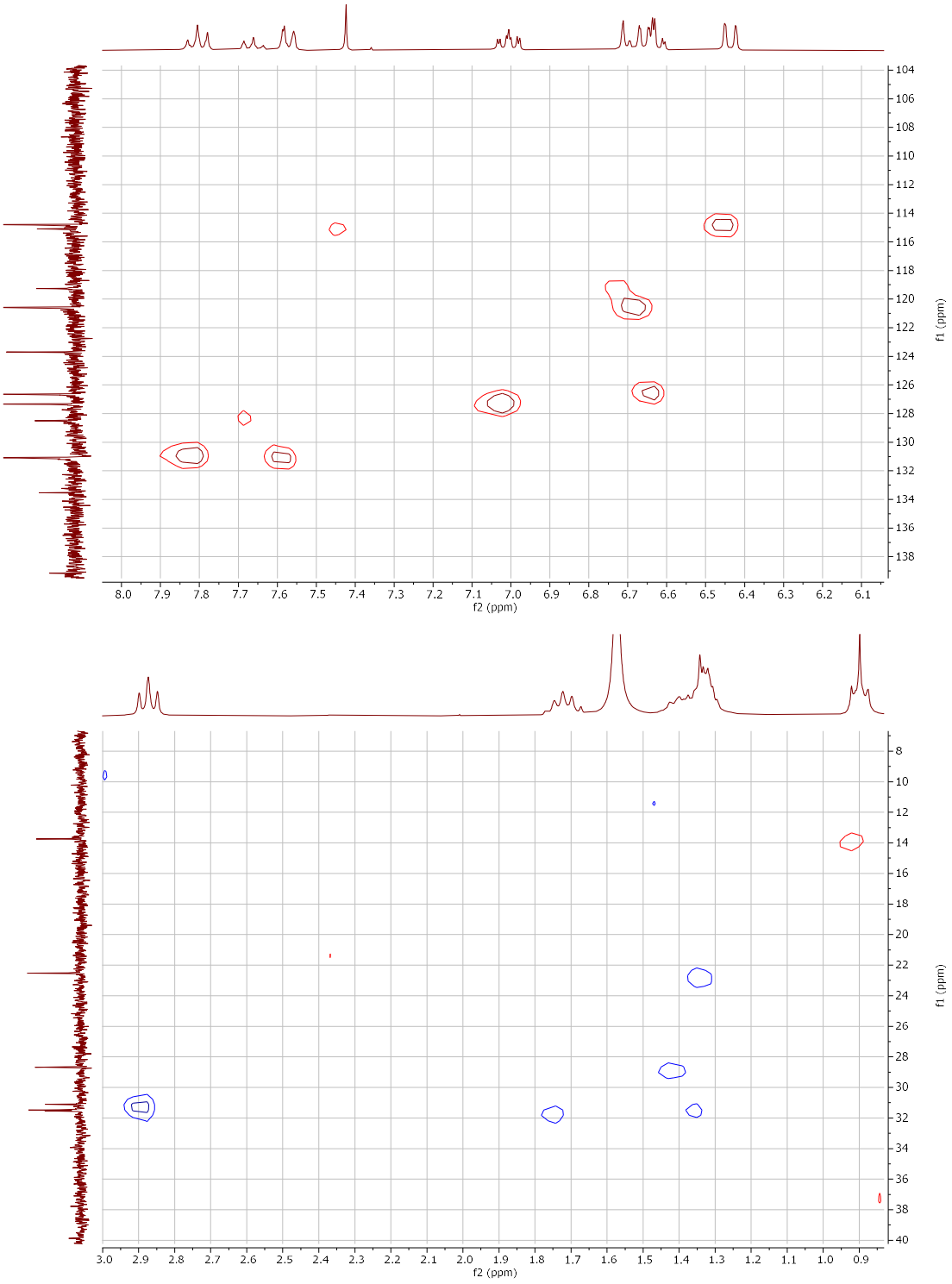

6.3.4 HMBC ***para*-DSPA-IDT**

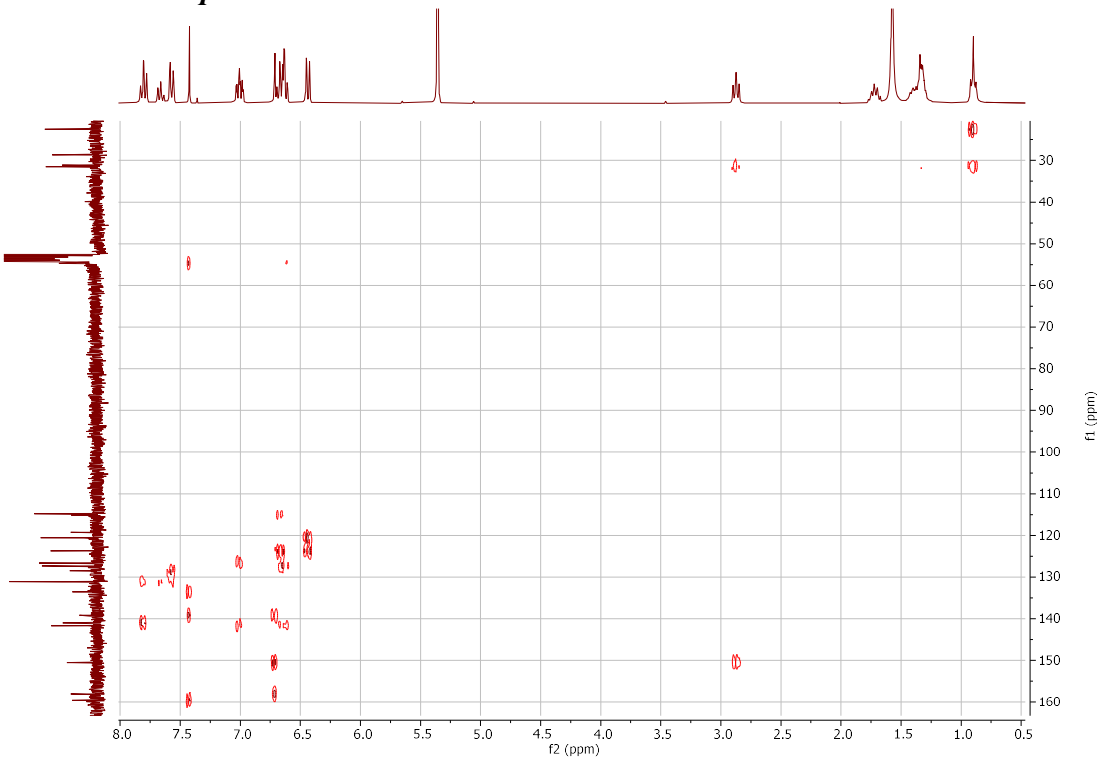

6.3.5 COSY ***para*-DSPA-IDT**

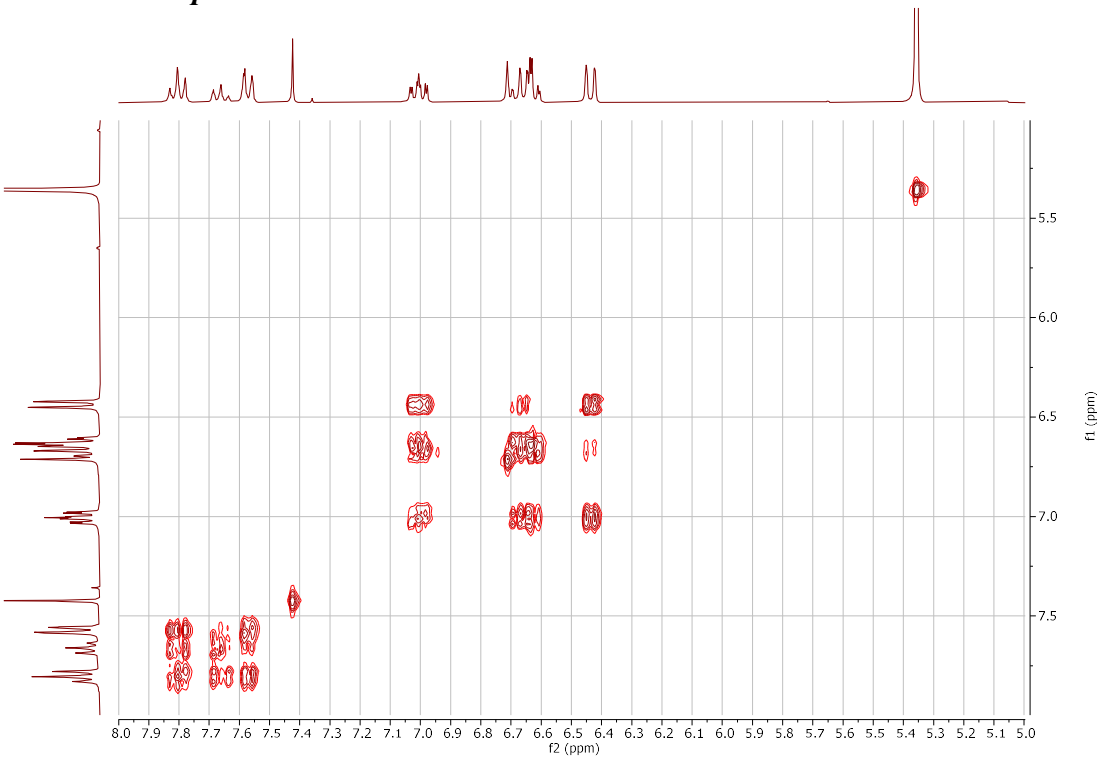

6.4 ***meta*-DSPA-IDT**

6.4.1 ^{1}H ***meta*-DSPA-IDT** in CD_2Cl_2

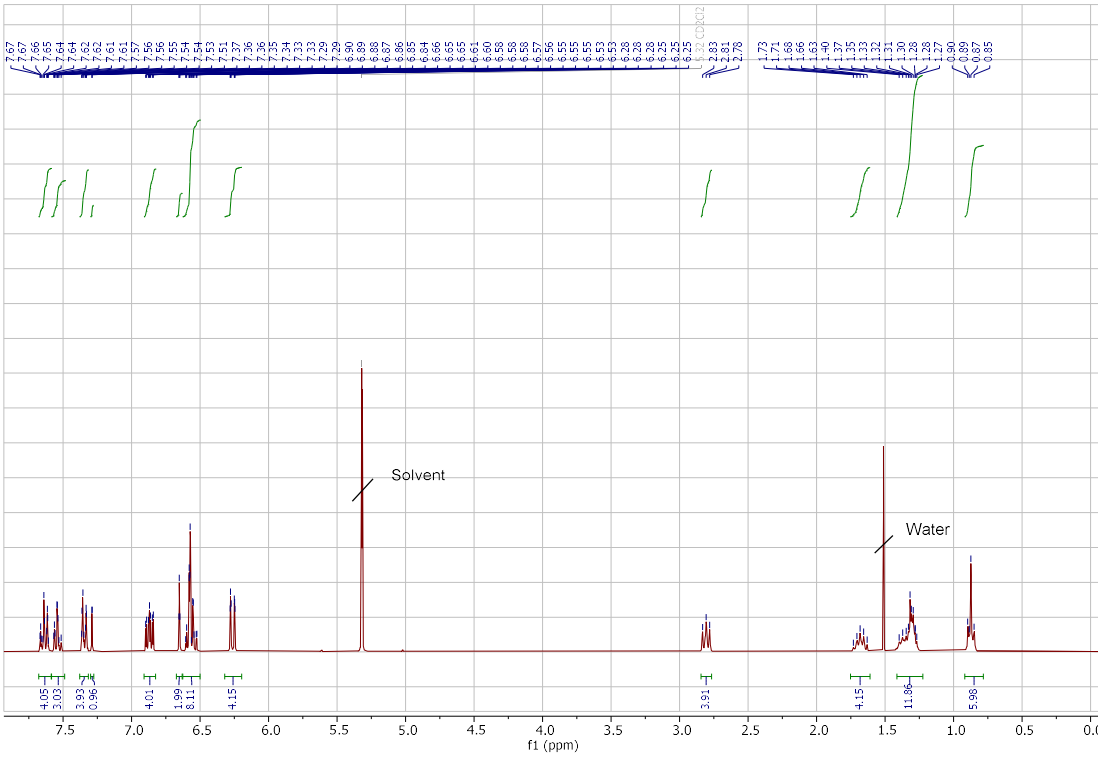

6.4.2 ^{13}C ***meta*-DSPA-IDT** in CD_2Cl_2

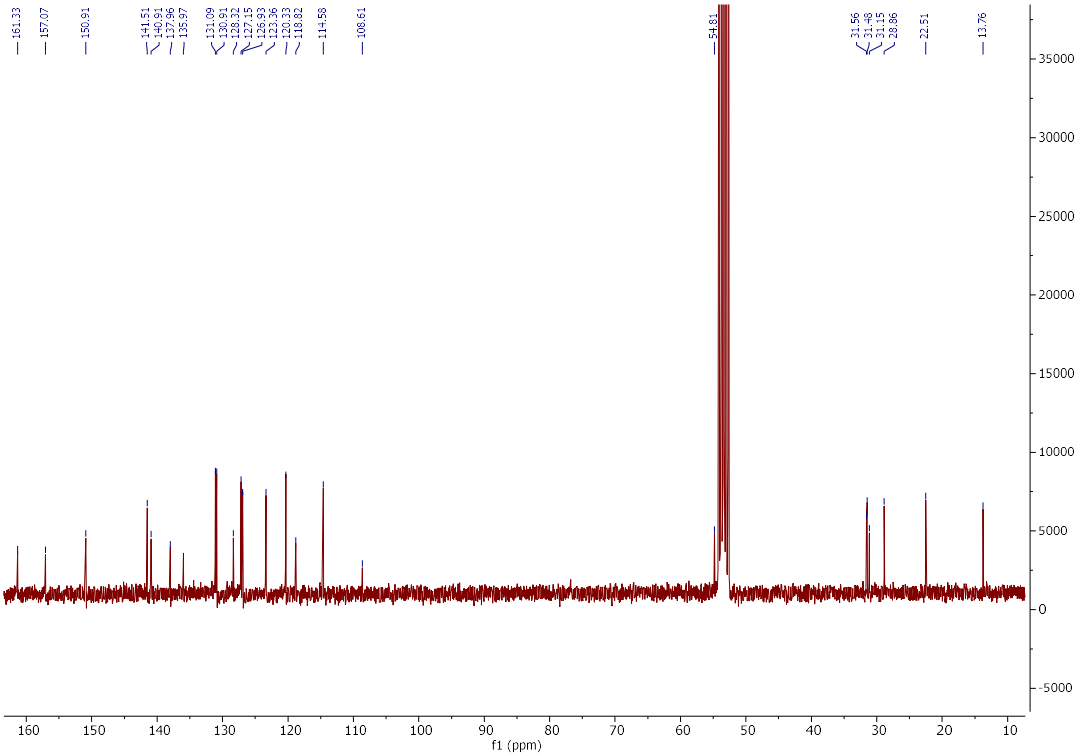

6.4.3 DEPT ***meta*-DSPA-IDT**

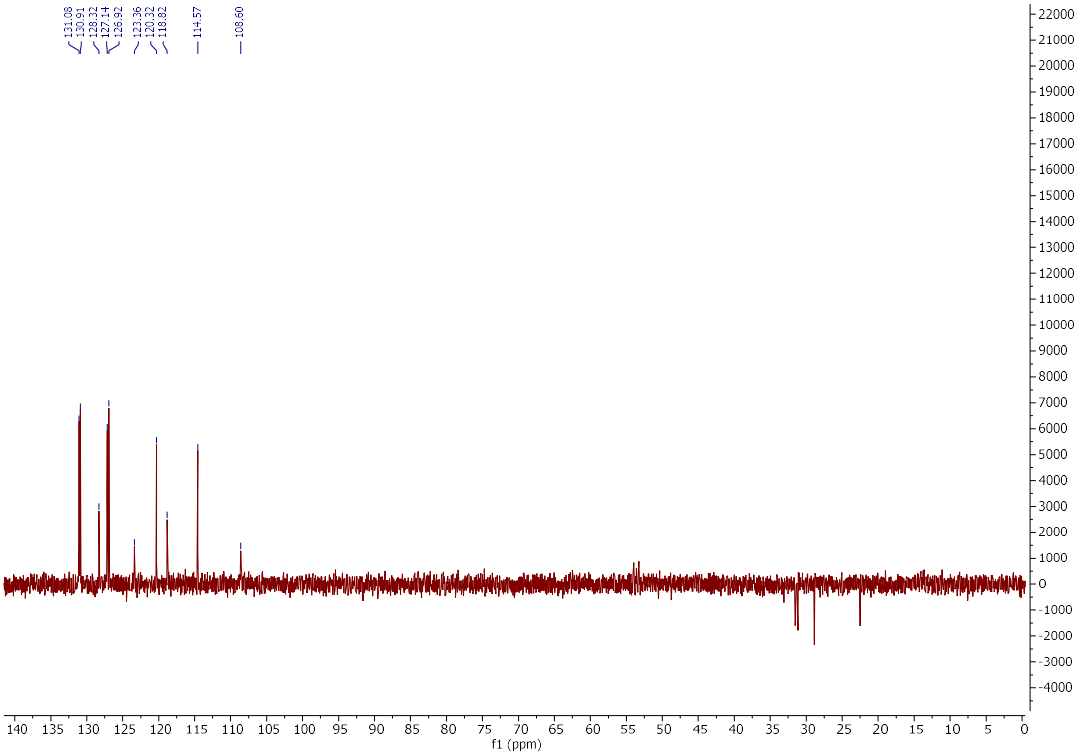

6.4.4 HSQC ***meta*-DSPA-IDT**

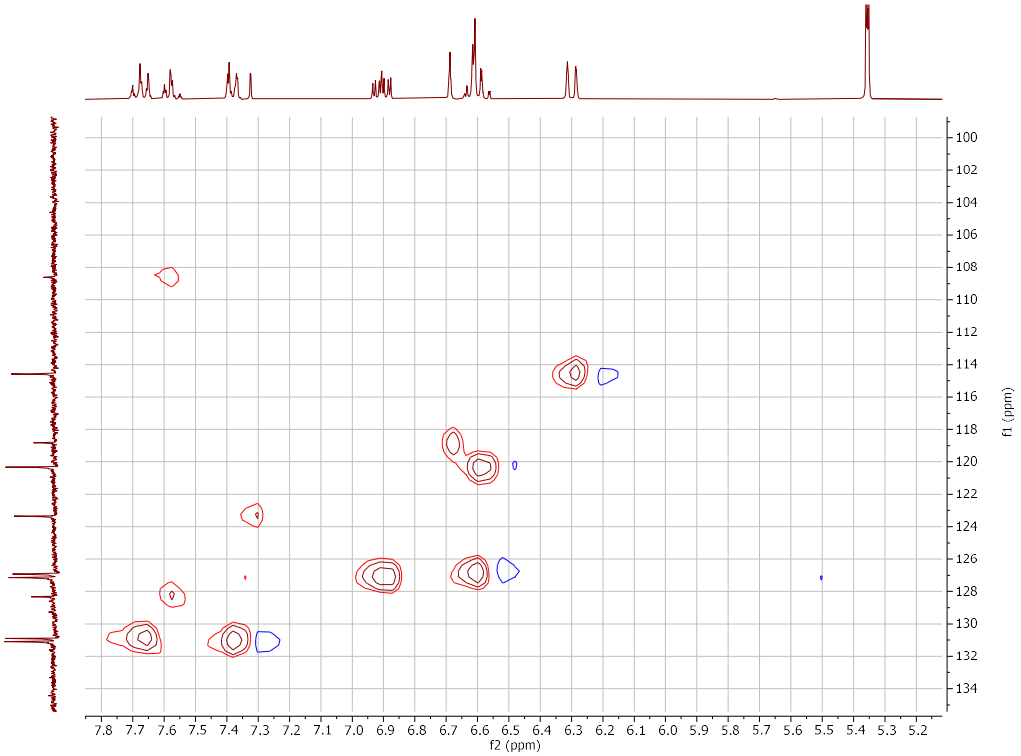

6.4.5 HMBC ***meta*-DSPA-IDT**

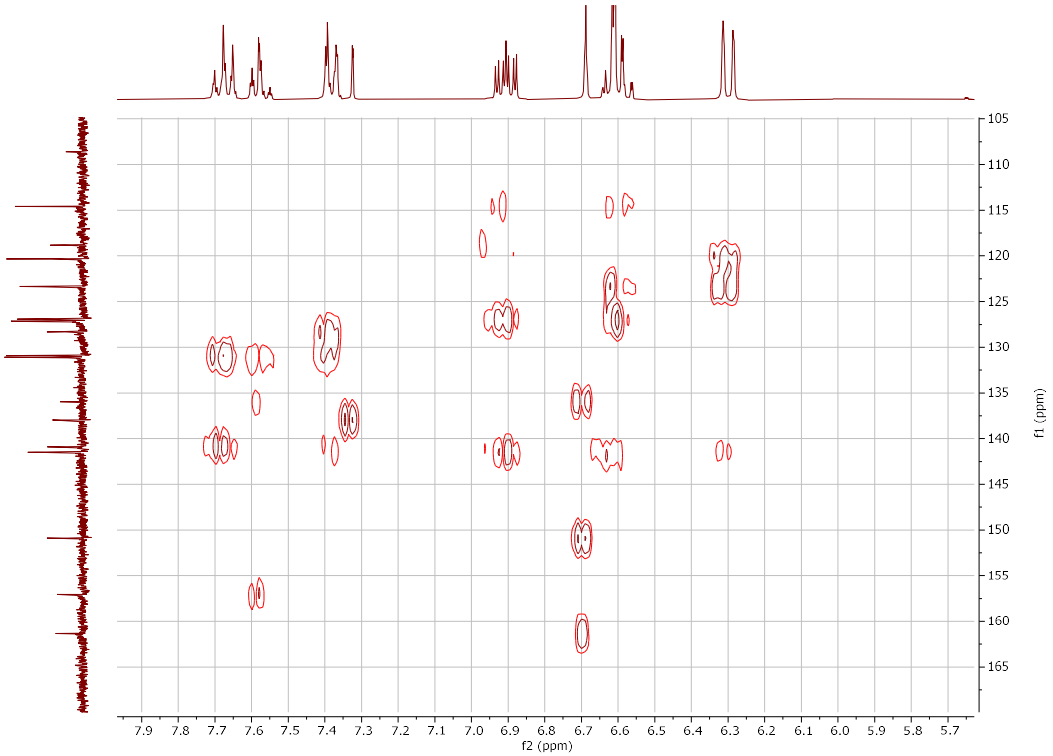

6.4.6 COSY ***meta*-DSPA-IDT**

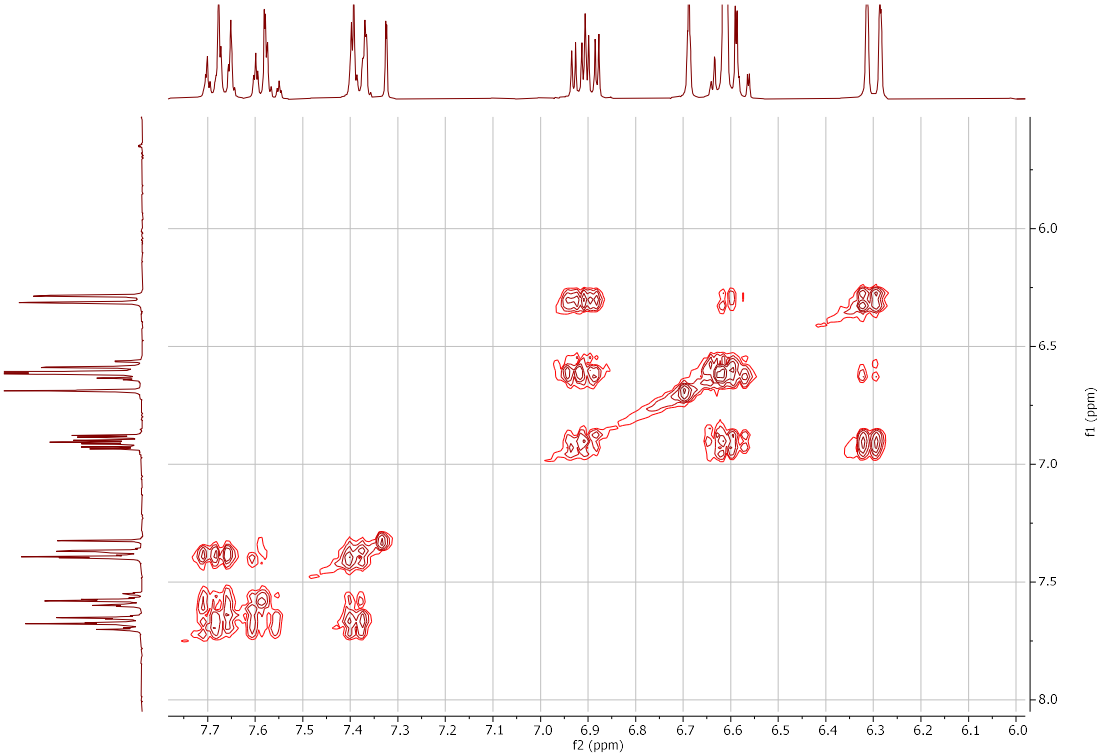

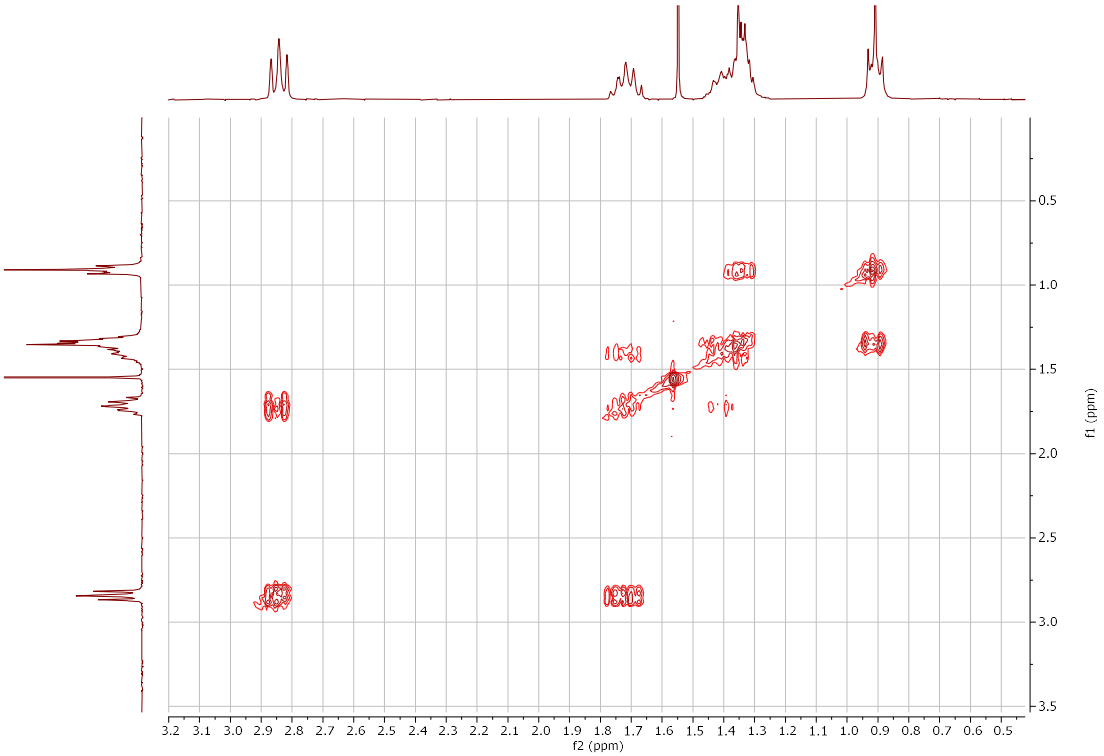

(1) Kulkarni, A. P.; Tonzola, C. J.; Babel, A.; Jenekhe, S. A. Electron Transport Materials for Organic Light-Emitting Diodes. *Chem. Mater.* **2004**, *16*, 4556–4573.

(2) Kohn, P. H. a. W. Inhomogeneous Electron Gas. *Phys. Rev.*, *136*, B864.

(3) Calais, J.-L. Density-Functional Theory of Atoms and Molecules. . *Int. J. Quant. Chem.* **1993**, *47*, 101.

(4) Becke, A. D. Density-functional exchange-energy approximation with correct asymptotic behavior. *Phys. Rev. A* **1988**, *38*, 3098.

(5) Becke, A. D. A new mixing of Hartree–Fock and local density-functional theories *J. Chem. Phys.* **1993**, *98*, 1372.

(6) Becke, A. D. Density-functional thermochemistry. III. The role of exact exchange *J. Chem. Phys.* **1993**, *98*, 5648.

(7) Lee C., Y. W. a. R. G. P. Development of the Colle-Salvetti correlation-energy formula into a functional of the electron density. *phys. rev. B* **1988**, *37*, 785.

(8) M. J. Frisch, G. W. T., H. B. Schlegel, G. E. Scuseria, M. A. Robb, J. R. Cheeseman, G. Scalmani, V. Barone, B. Mennucci, G. A. Petersson, H. Nakatsuji, M. Caricato, X. Li, H. P. Hratchian, A. F. Izmaylov, J. Bloino, G. Zheng, J. L. Sonnenberg, M. Hada, M. Ehara, K. Toyota, R. Fukuda, J. Hasegawa, M. Ishida, T. Nakajima, Y. Honda, O. Kitao, H. Nakai, T. Vreven, J. A. J. Montgomery, J. E. Peralta, F. Ogliaro, M. Bearpark, J. J. Heyd, E. Brothers, K. N. Kudin, V. N. Staroverov, T. Keith, R. Kobayashi, J. Normand, K. Raghavachari, A. Rendell, J. C. Burant, S. S. Iyengar, J. Tomasi, M. Cossi, N. Rega, J. M. Millam, M. Klene, J. E. Knox, J. B. Cross, V. Bakken, C. Adamo, J. Jaramillo, R. Gomperts, R. E. Stratmann, O. Yazyev, A. J. Austin, R. Cammi, C. Pomelli, J. W. Ochterski, R. L. Martin, K. Morokuma, V. G. Zakrzewski, G. A. Voth, P. Salvador, J. J. Dannenberg, S. Dapprich, A. D. Daniels, O. Farkas, J. B. Foresman, J. V. Ortiz, J. Cioslowski, D. J. Fox. **2010**, Gaussian 09, Revision B.01, Gaussian, Inc., Wallingford CT, 2010.

(9) Lucas, F.; Ibraikulov, O. A.; Quinton, C.; Sicard, L.; Heiser, T.; Tondelier, D.; Geffroy, B.; Leclerc, N.; Rault-Berthelot, J.; Poriel, C. Spirophenylacridine-2,7-(diphenylphosphineoxide)-fluorene: A Bipolar Host for High-Efficiency Single-Layer Blue Phosphorescent Organic Light-Emitting Diodes. *Adv. Opt. Mater.* **2020**, *8*, 1901225.

(10) Peltier, J.-D.; Heinrich, B.; Donnio, B.; Rault-Berthelot, J.; Jacques, E.; Poriel, C. Electron-Deficient Dihydroindaceno-Dithiophene Regioisomers for n-Type Organic Field-Effect Transistors. *ACS Appl. Mater. Interfaces* **2017**, *9*, 8219-8232.

(11) Merlet, S.; Birau, M.; Wang, Z. Y. Synthesis and characterization of highly fluorescent indenofluorenes. *Org. Lett.* **2002**, *4*, 2157-2159.